

Detrimental Effect of Impact Ionization in the Absorption Region on the Frequency Response and Excess Noise Performance of InGaAs–InAlAs SACM Avalanche Photodiodes

Ning Duan, S. Wang, X. G. Zheng, X. Li, Ning Li, Joe C. Campbell, *Fellow, IEEE*, Chad Wang, and Larry A. Coldren, *Fellow, IEEE*

Abstract—It is shown that optimization of the electric field profile in the absorption region of separate absorption, charge, and multiplication InGaAs–InAlAs avalanche photodiodes is critical to achieve low excess noise and high gain bandwidth product.

Index Terms—Avalanche photodiodes (APDs), excess noise factor, impact ionization, photodetectors.

I. INTRODUCTION

AVALANCHE photodiodes (APDs) are important components in many optical receivers due to the sensitivity margin provided by their internal gain. The separate absorption, charge, and multiplication (SACM) structure APD, which consists of an absorbing region and a multiplication region separated by a charge layer, has the advantage that the photon absorption process and the carrier multiplication process are independent and can be optimized individually to improve both the noise and speed performance [1]. Further, this structure effectively suppresses tunneling in the narrow bandgap-absorbing layer.

$\text{In}_{0.53}\text{Ga}_{0.47}\text{As}$ – $\text{In}_{0.52}\text{Al}_{0.48}\text{As}$ (referred to below as InGaAs and InAlAs) APDs have been studied for high-bit-rate optical communication applications [2], [3]. Reduction of the transit time in these APDs can be achieved by utilizing thin absorption layers [4]–[6]. For high responsivity in normal incidence APDs, however, a thick absorption layer is required (the quantum efficiency of a InGaAs–InAlAs SACM APDs with a 1.5- μm InGaAs absorption region is 13% higher than that with a 1- μm InGaAs absorption region), which results in a tradeoff between the sensitivity and the speed. Further, it has been shown for InP–InGaAs separate absorption and multiplication APDs that impact ionization in the absorption region, which is more pronounced for thick absorption regions, can significantly reduce the gain–bandwidth product [7]–[10]. In this paper, we study the speed and noise performance of InGaAs–InAlAs SACM APDs with a thick ($\sim 1.5 \mu\text{m}$) absorption region. We find that

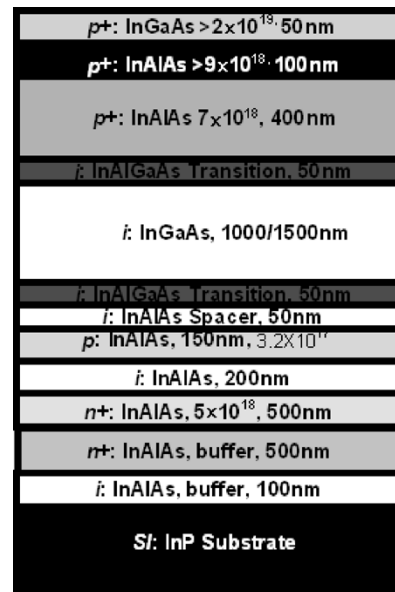


Fig. 1. Schematic layer structure of the InGaAs–InAlAs SACM APD.

the doping profile in the InGaAs absorption layer influences the level of impact ionization in that layer, which, in turn, significantly affects the gain–bandwidth product and the excess noise.

II. DEVICE STRUCTURE

The structures were grown in a molecular beam epitaxy reactor, on semi-insulating InP substrates. As shown in Fig. 1, the first layer grown was a 100-nm-thick unintentionally doped InAlAs layer to suppress silicon diffusion into the semi-insulating InP substrate from the InAlAs n-contact layer, which can cause excessive parasitic capacitance between contact pads. A 500-nm-thick heavily doped n^+ -type (silicon, $\geq 8 \times 10^{18} \text{ cm}^{-3}$) InAlAs layer was grown as a buffer layer and was followed by a 500-nm n^+ -type (silicon, $\geq 5 \times 10^{18} \text{ cm}^{-3}$) $\text{In}_{0.52}\text{Al}_{0.48}\text{As}$ contact layer. Following the n-type contact layer, was the multiplication region, an intrinsic InAlAs layer, with a thickness of 200 nm. Next to be deposited was the charge layer, 150-nm-thick p-type (Be-doped) $\text{In}_{0.52}\text{Al}_{0.48}\text{As}$. A 1000 or 1500-nm-thick intrinsic InGaAs, which was sandwiched between two 50-nm-thick unintentionally doped InAlAs spacer

Manuscript received September 30, 2004; revised December 6, 2004.

N. Duan, S. Wang, X. Li, N. Li, and J. C. Campbell are with the Department of Electrical and Computer Engineering, University of Texas at Austin, TX 78713 USA (e-mail: jcc@mail.utexas.edu).

X. G. Zheng is with JDS Uniphase, San Jose, CA 95134 USA.

C. Wang and L. A. Coldren are with the University of California at Santa Barbara, CA 93106 USA.

Digital Object Identifier 10.1109/JQE.2005.843613

TABLE I
PROPERTIES OF APD WAFERS

Parameter	Wafer A	Wafer B	Wafer C
Absorption layer thickness	1 μm	1.5 μm	1.5 μm
Absorption layer doping	Unintentional n-type background doping $2 \times 10^{15} \text{ cm}^{-3}$	Unintentional n-type background doping $2 \times 10^{15} \text{ cm}^{-3}$	p ⁻ doping of $5 \times 10^{15} \text{ cm}^{-3}$

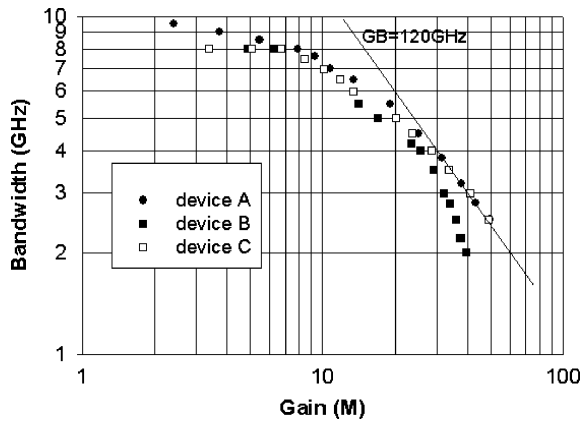


Fig. 2. Measured 3-dB bandwidth versus gain for devices A, B, and C.

layers, was grown as the absorbing layer. The 50-nm undoped InGaAlAs grading layers were inserted to reduce the barrier between InAlAs and InGaAs in order to prevent hole pile-up in the heterointerface. Then a 400-nm-thick p-type (Be-doped, $7 \times 10^{18} \text{ cm}^{-3}$) InAlAs window layer was grown. The p-type contact layers consisted of 100 nm of $\text{In}_{0.52}\text{Al}_{0.48}\text{As}$ (Be: $\geq 2 \times 10^{19} \text{ cm}^{-3}$) capped with 50 nm of InGaAs doped at the same level. The wafers studied are compared in Table I. SIMS measurements on all three wafers indicated that, within the measurement accuracy, the structures of wafers A, B, and C were as designed with the same charge doping level of $3.2 \times 10^{17} \text{ cm}^{-3}$. This was also confirmed with capacitance–voltage measurements.

The wafers were fabricated by wet chemical etching into back illuminated mesa structures with diameters in the range 20 to 50 μm . The 50- μm -diameter devices were chosen for speed and noise measurements. The mesas were passivated by plasma-enhanced chemical vapor deposition of SiO_2 . The passivation also served as a partial antireflection coating. Ti–Pt–Au metal dot contacts were deposited on the top p-surface of the mesa, and AuGe–Ni–Au contacts were deposited on the n-surface. Conventional photolithography and liftoff metallization techniques were used to define the metal contacts. Microwave contact pads with an air-bridge connection were fabricated for high-speed measurements.

III. RESULTS AND DISCUSSION

S21 Frequency response measurements were made on 50 μm -diameter devices at the wavelength of 1.3 μm . Fig. 2 shows the measured 3-dB bandwidth of devices A, B, and C. If avalanche multiplication is confined to the multiplication region, the gain–bandwidth product should be same for all three devices since they have the same multiplication region.

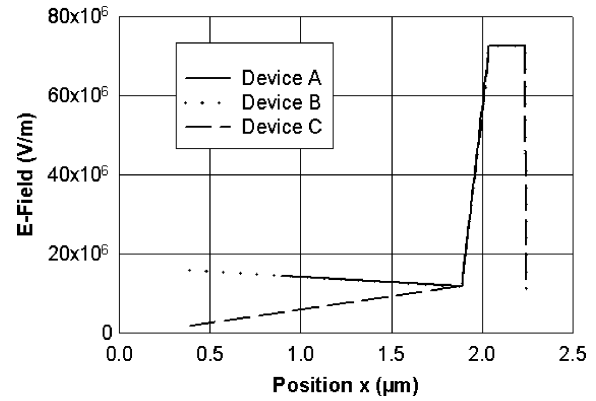


Fig. 3. One-dimensional electric-field profile of devices A, B, and C at gain of 20.

Devices A and C have the same gain–bandwidth product of 120 GHz, an indication that there is insignificant impact ionization in the absorbing layer for these two devices. However, for device B, the bandwidth begins to drop at $M = 15$. This bandwidth degradation compared to devices A and C is due to impact ionization in the thick InGaAs absorption region. In the SACM structure, a high electric field in the multiplication region is required to provide gain, whereas the electric field intensity in the absorbing layer is required to be sufficiently low so as 1) to suppress tunneling and 2) to minimize carrier multiplication in the absorbing region, which is extremely detrimental to APD speed performance [7]–[10]. The electric field strength that causes significant low field carrier multiplication in InGaAs is approximately 150 kV/cm [11], whereas the threshold for tunneling is approximately 220 kV/cm. This speed degradation for device B can be explained by the electric field profile in the absorption region (Fig. 3). The n-type background doping in device B contributes to an electric field profile in which the field in the absorption region closer to the top surface is higher than at the side near the charge layer. When the gain exceeds ~ 15 , the electrical field in the absorption region of device B is $\sim 150 \text{ kV/cm}$. With further increase in the electric field, impact ionization becomes more and more significant. Hence, the n-type background doping leads to impact ionization in the portion of the absorption region closer to the top surface where the electric field is higher, which can be extremely detrimental to the speed owing to the effective increase in the total multiplication width for a fraction of the carriers. If the impact ionization in the absorption region occurs in the region near the multiplication region, the speed degradation will not be as serious.

To reduce this bandwidth degradation, we have introduced a p⁻ doping of $5 \times 10^{15} \text{ cm}^{-3}$ in the absorption region of device C in order to keep the electric field low. From Fig. 2 it can be seen that, for device C, the bandwidth for $30 < M < 50$ fits the line of 120-GHz gain–bandwidth product. There is no bandwidth drop similar to that observed for device B, a reflection of the fact that the electrical field in the absorption region of device C remains low ($< 150 \text{ kV/cm}$) up to a gain of 50 due to the p⁻ doping as shown in Fig. 3. Although the electric field profile

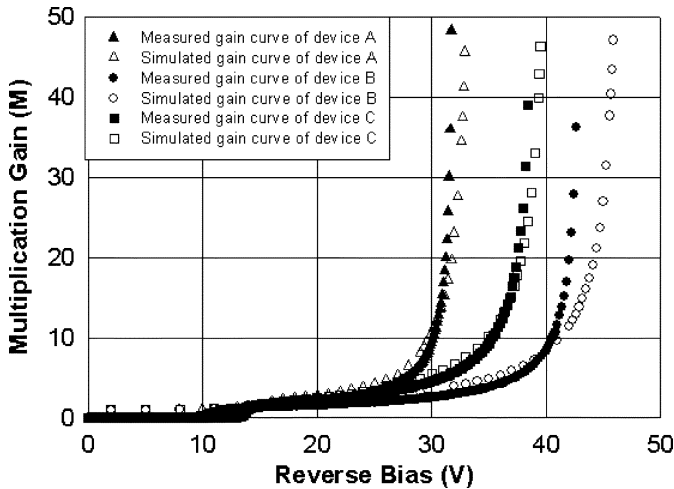


Fig. 4. Measured and simulated gain as a function of reverse bias voltage for devices A, B, and C.

of device A is the same as that of device B, there is no significant bandwidth degradation for device A since its absorption region is $0.5 \mu\text{m}$ thinner than B. Hence, the maximum electric field value in the absorbing region of device A is not as high as that of device B as shown in Fig. 3. The degree of impact ionization is proportional to the product of ionization coefficient and available multiplication width (nonlocal theory). Device A has both lower ionization coefficient and multiplication width.

The gain–bandwidth products of devices A and C are 120 GHz. This value is consistent with previously published results for APDs with similar InAlAs multiplication layer thickness [12]. Devices A and C have the same gain–bandwidth product since they have the same 200-nm-thick InAlAs multiplication region. In the low gain regime, the bandwidth of device A is 9 GHz, while that of device C is 8 GHz. The RC limited bandwidth was estimated by measuring the S11 parameters with a network analyzer. The measured capacitance was ~ 150 fF and total resistance was $\sim 70 \Omega$, yielding an estimated RC-bandwidth of 15 GHz. This frequency is too high to account for the observed 8- and 9-GHz ceilings. The carrier transit-time bandwidth is 13 GHz for devices B and C and 17 GHz for device A if there are no secondary carriers [13]. But for this case, the transit time for the secondary holes to traverse the whole depletion region is important. (The secondary electrons can be neglected since the absorbing layer is much wider than the multiplication region). Taking the transit time of secondary holes into effect, the transit time is ~ 7 ps for devices B and C and ~ 6 ps for device A. Hence we conclude that the observed low gain bandwidths of 8 and 9 GHz are determined by the hole transit time [14]. In the high gain regime ($M > 30$), the bandwidth is dominated by the avalanche buildup time.

According to Emmons' model [15], in the high gain regime, the effective transit time for devices A and C is 1.3 ps.

Using the analytical model described in [16], we simulated the gain curves of devices A, B, and C (Fig. 4). The gain curves were measured using the procedure described in [12]. The measured gain curve of device B is sharper than the simulated gain curve since the simulation assumes no impact ionization in the

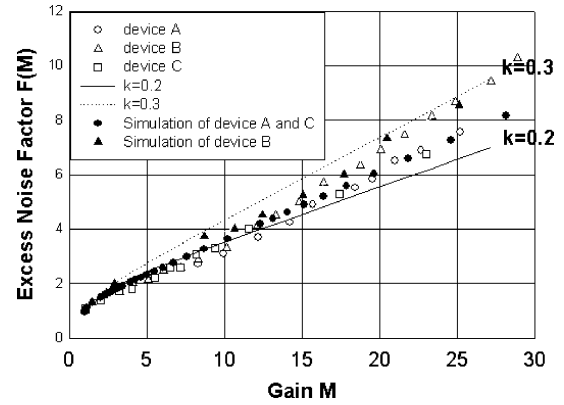


Fig. 5. Simulated and experimental excess noise factor as a function of gain for devices A, B, and C.

absorption region, which causes the gain to increase faster. The gain value contributed by a $1.5\text{-}\mu\text{m}$ -thick InGaAs absorbing layer with an electric field of 150 kV/cm is calculated to be 1.13 using the parameters and equations given by [10]. This calculated gain result is consistent with the measured result of [11]. From [17], if a small fraction ε of the secondary holes traveling back across the absorber initiate impact ionization in the absorption region, the total gain is given by

$$M = \frac{M_0}{[1 - \varepsilon(M_0 - 1)]} \quad (1)$$

where M_0 is the electron initiated gain of the InAlAs avalanche region and ε is the feedback factor. At a bias of 42 V as shown in Fig. 4, the measured gain M of device B is 30, while the simulated gain M_0 is 15. The simulated gain of 15 is the gain from the InAlAs multiplication region. Hence, we estimated that the feedback factor ε at this point is 0.036. This shows that if only 3.6% of the secondary holes that traverse the absorbing layer initiate impact ionization, the gain will increase by a factor of two. On the other hand, for devices A and C, the simulated and measured gain curves are coincident. The estimated values of ε are 0.01 and 0.007 for devices A and C, respectively. The small feedback factors for devices A and C explain why there is no bandwidth degradation for these two devices.

To further study the effect of ionization in the absorption layer, the excess noise factor $F(M)$ of these APDs was measured using the procedure described in [18]. A tunable laser operating at $1.55 \mu\text{m}$ was used as the light source for these measurements. The measured $F(M)$ of devices A, B, and C are shown in Fig. 5. The effective k value was estimated to be 0.2 for both devices A and C. This value is consistent with previously published results for a SACM APD with similar thickness InAlAs multiplication region [19]. The black circle is the simulated $F(M)$ of device A and C using the analytical model described in [16], assuming that impact ionization is confined to the multiplication region. The excess noise of devices A and C follows the simulation. On the other hand, for $M > 15$, the excess noise of device B deviates from the $k = 0.2$ curve, further confirmation that there is impact ionization in the absorption region. A Monte Carlo simulation [20] confirmed that significant impact ionization occurs in the InGaAs absorption layer;

the simulated noise curve for device B is marked by black triangles in Fig. 5.

In conclusion, we have demonstrated the detrimental effect of impact ionization in the absorption region on the speed and noise performance of InGaAs–InAlAs SACM APDs. We find that the doping profile in the absorption layer strongly influences the amount of impact ionization and thus the gain–bandwidth product and the excess noise.

REFERENCES

- [1] H. Nie, K. A. Anselm, C. Hu, S. S. Murtaza, B. G. Streetman, and J. C. Campbell, "High-speed resonant-cavity separate absorption and multiplication avalanche photodiodes with 130 GHz gain-bandwidth product," *Appl. Phys. Lett.*, vol. 70, pp. 161–163, Jan. 1997.
- [2] T. Nakata, T. Takeuchi, J. Watanabe, K. Makita, and T. Torikai, "10 Gbit/s high sensitivity, low-voltage-operation avalanche photodiodes with thin InAlAs multiplication layer and waveguide structure," *Electron. Lett.*, vol. 36, pp. 2033–2034, Nov. 2000.
- [3] C. Lenox, H. Nie, P. Yuan, G. Kinsey, A. L. Holmes Jr., B. G. Streetman, and J. C. Campbell, "Resonant-cavity InGaAs–InAlAs avalanche photodiodes with gain-bandwidth product of 290 GHz," *IEEE Photon. Technol. Lett.*, vol. 11, no. 9, pp. 1162–1164, Sep. 1999.
- [4] G. S. Kinsey, J. C. Campbell, and A. G. Dentai, "Waveguide avalanche photodiode operating at 1.55 μm with a gain-bandwidth product of 320 GHz," *IEEE Photon. Technol. Lett.*, vol. 13, no. 8, pp. 842–844, Aug. 2001.
- [5] S. Demiguel, N. Li, X. Li, X. Zheng, J. Kim, J. C. Campbell, H. Lu, and A. Anselm, "Very high-responsivity evanescently coupled photodiodes integrating a short planar multimode waveguide for high-speed applications," *IEEE Photon. Technol. Lett.*, vol. 15, no. 12, pp. 1761–1703, Dec. 2003.
- [6] J. Wei, F. Xia, and S. R. Forrest, "A high-responsivity high-bandwidth asymmetric twin-waveguide coupled InGaAs–InP–InAlAs avalanche photodiode," *IEEE Photon. Technol. Lett.*, vol. 14, no. 11, pp. 1590–1592, Nov. 2002.
- [7] I. Watanabe, M. Tsuji, K. Makita, and K. Taguchi, "Gain-Bandwidth product analysis of InAlGaAs–InAlAs superlattice avalanche photodiodes," *IEEE Photon. Technol. Lett.*, vol. 8, no. 2, pp. 269–271, Feb. 1996.
- [8] L. E. Tarof, J. Yu, R. Bruce, D. G. Knight, T. Baird, and B. Oosterbrink, "High-Frequency performance of separate absorption, grading, charge, and multiplication InP/InGaAs avalanche photodiodes," *IEEE Photon. Technol. Lett.*, vol. 5, no. 6, pp. 672–674, Jun. 1993.
- [9] G. Kahraman, N. E. A. Saleh, W. L. Sargeant, and M. C. Teich, "Time and frequency response of avalanche photodiodes with arbitrary structure," *IEEE Trans. Electron Devices*, vol. 39, no. 3, pp. 553–560, Mar. 1992.
- [10] F. Osaka and T. Mikawa, "Excess noise design of InP–GaInAsP–GaInAs avalanche photodiodes," *IEEE J. Quantum Electron.*, vol. QE-22, no. 3, pp. 471–478, Mar. 1986.
- [11] J. S. Ng, C. H. Tan, J. P. R. David, G. Hill, and G. J. Rees, "Dependence of impact ionization coefficients in $\text{In}_{0.53}\text{Ga}_{0.47}\text{As}$," *IEEE Trans. Electron Devices*, vol. 50, no. 4, pp. 901–906, Apr. 2003.
- [12] X. G. Zheng, J. S. Hsu, J. B. Hurst, X. Li, S. Wang, X. Sun, A. L. Holmes Jr., J. C. Campbell, A. S. Huntington, and L. A. Goldren, "Long-wavelength InGaAs–InAlAs large-area avalanche photodiodes and arrays," *IEEE J. Quantum Electron.*, vol. 40, no. 8, pp. 1068–1073, Aug. 2004.
- [13] K. Kato, "Ultrawide-band/high-frequency photodetectors," *IEEE Trans. Microwave Theory Tech.*, vol. 47, no. 7, pp. 1265–1281, Jul. 1999.
- [14] J. C. Campbell, W. T. Tsang, G. J. Qua, and B. C. Johnson, "High speed InP–InGaAsP–InGaAs avalanche photodiodes grown by chemical beam epitaxy," *IEEE J. Quantum Electron.*, vol. 24, no. 3, pp. 496–500, Mar. 1988.
- [15] E. B. Emmons, "Avalanche-photodiode frequency response," *J. Appl. Phys.*, vol. 38, pp. 3705–3714, Aug. 1967.
- [16] X. Li, X. Zheng, S. Wang, F. Ma, and J. C. Campbell, "Calculation of gain and noise with dead space for GaAs and $\text{Al}_x\text{Ga}_{1-x}\text{As}$ avalanche photodiode," *IEEE Trans. Electron Devices*, vol. 49, no. 7, pp. 1112–1117, Jul. 2002.

- [17] J. N. Holenhorst, D. T. Ekholm, J. M. Geary, V. D. Mattered Jr., and R. Pawelek, "High frequency performance of planar InGaAs/InP avalanche photodiodes," *Proc. SPIE*, vol. 995, p. 53, Sep. 1988.
- [18] S. Wang, R. Sidhu, X. G. Zheng, X. Li, X. Sun, A. L. Holmes Jr., and J. C. Campbell, "Low-noise avalanche photodiodes with graded impact-ionization-engineered multiplication region," *IEEE Photon. Technol. Lett.*, vol. 13, no. 12, pp. 1346–1348, Dec. 2001.
- [19] N. Li, R. Sidhu, X. Li, F. Ma, X. Zheng, S. Wang, G. Karve, S. Demiguel, A. L. Holmes Jr., and J. C. Campbell, "InGaAs/InAlAs avalanche photodiode with undepleted absorber," *Appl. Phys. Lett.*, vol. 82, pp. 2175–2177, Mar. 2003.
- [20] F. Ma, N. Li, and J. C. Campbell, "Monte Carlo simulation of the bandwidth of InAlAs avalanche photodiodes," *IEEE Trans. Electron Devices*, vol. 50, no. 11, pp. 2291–2294, Nov. 2001.

Ning Duan was born in Neimenggu, China, in 1978. She received the B.S. degree in applied physics and the M.S. degree in optics from Northern Jiaotong University, Beijing, China, in 1999 and 2001, respectively. She is currently working toward the Ph.D. degree in electrical engineering at the Microelectronic Research Center, University of Texas at Austin.

Her research interests are high-speed long-wavelength avalanche photodiodes and high-saturation power p-i-n photodiodes.



Electro-Optics Society.

S. Wang received the B.S. degree in microelectronics from Beijing University, China, in 1995 and the M.S.E.E. degree from University of Notre Dame, South Bend, IN, in 1999. She received the Ph.D. degree in electrical engineering from the University of Texas at Austin in 2002.

She is currently a Research Scientist in the Microelectronics Research Center at the University of Texas working on high-speed, low-noise avalanche photodiodes.

Dr. Wang is a member of the IEEE Lasers and



X. G. Zheng received the B.S.E.E. degree from the Beijing Institute of Technology, Beijing, China, in 1985 and the M.S. degree in electrical engineering from the Hebei Semiconductor Research Institute, Hebei, China, in 1991. He received the Ph.D. degree in electrical engineering from the University of Texas at Austin in 2004.

His major research interests are in optoelectronic devices: impact ionization properties of III-V compound materials, high-speed long-wavelength avalanche photodiodes and arrays, and heterogeneous material integration via direct wafer bonding. He is presently employed by JDS Uniphase, San Jose, CA.



X. Li was born in Beijing, China, in 1970. He received the B.S. and M.S. degrees from the Physics Department of Peking University, Beijing, China, in 1994 and 1997, respectively. He received the Ph.D. degree in electrical engineering from the Microelectronic Research Center, University of Texas at Austin in 2004.

His research interests are avalanche process simulations and high saturation power photodetectors for 1.55 μm applications. He is currently working for Applied Materials, University of Texas at Austin.



Ning Li was born in Beijing, China, in 1978. He received the B.S. and M.S. degrees from the Electronic Engineering Department, Tsinghua University, Beijing, China, in 1998 and 2000, respectively. He is currently pursuing the Ph.D. degree in electrical engineering at the Microelectronic Research Center, University of Texas at Austin.

His research interests are waveguide p-i-n and APD photodetectors.



Joe C. Campbell (S'73–M'74–SM'88–F'90) received the B.S. degree in physics from The University of Texas at Austin in 1969 and the M.S. and Ph.D. degrees in physics from the University of Illinois at Urbana-Champaign in 1971 and 1973, respectively.

From 1974 to 1976, he was with Texas Instruments Incorporated, Dallas, TX, where he was involved with integrated optics. In 1976, he joined the staff of AT&T Bell Laboratories, Holmdel, NJ. In the Crawford Hill Laboratory, he worked on a variety

of optoelectronic devices including semiconductor lasers, optical modulators, waveguide switches, photonic integrated circuits, and photodetectors with emphasis on high-speed avalanche photodiodes for high-bit-rate lightwave systems. In January 1989, he joined the faculty of The University of Texas at Austin as a Professor of Electrical and Computer Engineering and Cockrell Family Regents Chair in Engineering. At present, he is actively involved in Si-based optoelectronics, high-speed, low-noise avalanche photodiodes, high-power photodiodes, ultraviolet photodetectors, and quantum-dot IR imaging. He has coauthored six book chapters, more than 300 journal publications, and 200 conference presentations.

Prof. Campbell is a member of the National Academy of Engineering, a Fellow of the Optical Society of America, and a Fellow of the American Physical Society.

Chad Wang received the B.S. degree in electrical and computer engineering from the University of Texas at Austin in 2001. He is currently pursuing the Ph.D. degree at the University of California at Santa Barbara.

He is currently working on a novel, high-speed laser-modulator designed for optical interconnects. He is also involved in MBE growth of GaAs material and lattice-matched arsenides to InP for long-wavelength VCSELs and APDs.



Larry A. Coldren (S'67–M'72–SM'77–F'82) received the Ph.D. degree in electrical engineering from Stanford University, Stanford, CA, in 1972.

After 13 years in the research area at Bell Laboratories, he was appointed Professor of Electrical and Computer Engineering at the University of California at Santa Barbara (UCSB) campus in 1984. In 1986, he assumed a joint appointment with Materials and ECE, and in 2000 the Fred Kavli Chair in Optoelectronics and Sensors. He is also Chairman and Chief Technology Officer of Agility Communications, Inc.

At UCSB, his efforts have included work on novel guided-wave and vertical-cavity modulators and lasers as well as the underlying materials growth and fabrication technology. He is now investigating the integration of various optoelectronic devices, including optical amplifiers and modulators, tunable lasers, wavelength-converters, and surface-emitting lasers. He has authored or coauthored over 500 papers, five book chapters, one textbook, and has been issued 32 patents.

Prof. Coldren is a Fellow of the Optical Society of America (OSA) and a past Vice-President of IEEE Laser and Electro-Optics Society (LEOS).